$HCO(CH_2)_{10}CONHOH$, 103682-93-5; $MeONHCO(CH_2)_7CONHOMe$, 103682-96-8; $MeONHCO(CH_2)_8CONHOMe$, 103682-97-9; $MeONHCO(CH_2)_{10}CONHOMe$, 103835-51-4; $HONMeCO(CH_2)_7CONMeOH$, 103682-94-6; $HONMeCO(CH_2)_8CONMeOH$, 99102-77-9; $NiL\cdot H_2O$ (n = 5), 103835-53-6; $CuL\cdot H_2O$ (n = 5), 103835-54-7; $NiL\cdot H_2O$ (n = 10), 103835-55-8; glutaric acid, 110-94-1; *N,N'*-carbonyldiimidazole, 530-62-1; hydroxylamine, 7803-49-8; glutaric acid diimidazolide, 103835-52-5.

Contribution from the Institute of Inorganic Chemistry, University of Trondheim, N-7034 Trondheim-NTH, Norway

Successive High-Temperature Chlorine Substitution and Infrared Matrix-Isolation Spectroscopy of Methylaluminum Chlorides

Erling Rytter* and Steinar Kvisle[1]

Received June 12, 1985

Infrared spectra of the monomers $(CH_3)_2AlCl$ and $(CH_3)AlCl_2$ have been obtained by thermal dissociation of the corresponding dimers followed by isolation in argon matrices. The Al–C bond is found to be of similar stability for all monomers $(CH_3)_{3-n}AlCl_n$ (n = 0–2) while the strength of the Al–Cl bond decreases with higher alkyl contents. Several chlorine-bridged dimers, $(CH_3)_{6-n}Al_2Cl_n$ (n = 2–6), were identified in studies of dimeric dimethylaluminum chloride and methylaluminum dichloride. The experiments included elevated Knudsen cell temperatures, causing the following decompositions to occur: $(CH_3)_4Al_2Cl_2 \rightarrow (CH_3)_3AlCl_3 \rightarrow$ *trans*-$(CH_3)_2Al_2Cl_4$ (350–450 °C) and $(CH_3)_2Al_2Cl_4 \rightarrow (CH_3)Al_2Cl_5 \rightarrow Al_2Cl_6$ (550 °C). These cracking reactions are more prominent than the mere dissociations. On the basis of the valence force field of Al_2Cl_6 a good agreement between calculated and observed skeletal frequencies was achieved for the dimers. Frequencies were found to fall within narrow ranges for skeletal stretching modes involving the same atoms or groups.

Introduction

Aluminum alkyls and the related chlorides are essential components in Ziegler–Natta catalysts for the polymerization of propene.[2] Although these alkyls are important industrial chemicals, the knowledge on their structure and reactivity is relatively scarce. In this context, spectroscopic characterization is important, particularly if it is possible to prepare compounds with successive substitution of chlorine for alkyls. Group frequencies, relative bond strengths, and inductive effects then may be evaluated.

The most feasible possibility seems to be to produce the desired new compounds by high-temperature gas-phase experiments. Cracking reactions, dissociation of dimers and redistribution among alkyls and chlorine atoms may take place under these conditions. The products may be unstable and difficult to identify at high temperature, but immediate condensation with an inert material at cryogenic temperature allows the species to be studied carefully.

In a previous paper we reported the first infrared (IR) spectra of trimethyl- and triethylaluminum isolated in solid argon.[3] Matrices containing the monomers of these aluminum trialkyls were prepared by thermal dissociation of the dimers via the Knudsen cell technique. The dissociations were obtained without significant side reactions.

The chlorine-bridged dimeric structure of $(CH_3)_2AlCl$ and CH_3AlCl_2 has been confirmed by various spectroscopic methods,[4] including IR spectroscopy.[5-9] Vibrational data have, however, not been reported for the monomeric compounds and spectroscopic data are incomplete even for the dimers. This deficiency probably is due to experimental problems as the compounds are very reactive and hence difficult to handle. Furthermore, thermal dissociation of the dimers might be expected to be more difficult for the chlorides than for the pure aluminum alkyls as the chlorine bridge is stronger than the alkyl bridge.[10,11]

Here, we discuss the reactions of dimethylaluminum chloride (DMAC) and methylaluminum dichloride (MADC) at temperatures up to 550 °C. By the use of the Knudsen cell technique in conjunction with matrix isolation, reaction products could be isolated and characterized by IR spectroscopy. Interpretation of the vast amount of data gathered for different reaction temperatures and matrix-annealing times benefitted from normal coordinate analyses of the skeletal modes. A single dynamic model for alkyl groups and accurate force constants transferred from similar molecules constitute an effective tool in the identification and vibrational assignment of halogen-bridged compounds.

Experimental Section

The matrix-isolation apparatus has been described in detail elsewhere.[3,12] It consists of a closed-cycle helium cryostat (Cryodyne Cryocooler Model 21, CTI), a Pfeiffer TSU 110 turbomolecular pump, a stainless-steel deposition chamber equipped with CsI windows, a furnace, and a gas-mixing system. The inner stainless-steel tube of the furnace is sealed to the deposition chamber. Knudsen effusion cells of Graph-I-Tite G with an orifice diameter of 0.3 mm were employed. The temperature was measured with a Chromel/Alumel thermocouple connected to a Eurotherm proportional controller.

To avoid water and oxygen in the system, all parts were heated during evacuation, cooled and exposed in trimethylaluminum, and evacuated to 5×10^{-6} Torr before the deposition chamber was closed off from the pump.

Matrices were prepared by mixing the species leaving the Knudsen cell with argon gas immediately before the deposition window. The alkylaluminum chlorides were let into the Knudsen cell through a stainless-steel tube from a glass bulb attached to the furnace. The vapor pressure of the compound in the bulb was controlled by the temperature. Applied temperatures were 0 and 25 °C for DMAC and MADC, respectively, giving estimated vapor pressures of ca. 2–3 Torr.[13] Argon deposition rates were in the range 2–15 mmol/h, deposition times were 45 min, and

(1) Present address: Center for Industrial Research, 0314 Oslo 3, Norway.
(2) Boor, J. *Ziegler-Natta Catalysts and Polymerizations*; Academic: New York, 1979.
(3) Kvisle, S.; Rytter, E. *Spectrochim. Acta, Part A* **1984**, *40A*, 939.
(4) Mole, T.; Jeffery, E. A. *Organoaluminium Compounds*; Elsevier: Amsterdam, 1972, and references therein.
(5) Hoffmann, E. G. *Z. Elektrochem.* **1960**, *64*, 616.
(6) Groenewege, M. P. *Z. Phys. Chem. (Munich)* **1958**, *18*, 147.
(7) Gray, A. P. *Can. J. Chem.* **1963**, *41*, 1511.
(8) Onishi, T.; Shimanouchi, T. *Spectrochim. Acta* **1964**, *20*, 325.
(9) Weidlein, J. *J. Organomet. Chem.* **1969**, *17*, 213.
(10) *JANAF Thermochemical Tables*, 2nd ed.; NSRDS-NBS 37; U.S. Department of Commerce: Washington, D.C., 1971.
(11) Smith, M. B. *J. Organometal. Chem.* **1972**, *46*, 31.
(12) Kvisle, S.; Rytter, E. *J. Mol. Struct.* **1984**, *117*, 51.
(13) (a) *Aluminum Alkyls*; Texas Alkyls: Westport, TX, 1976. (b) Ufnalski, W.; Sporzynski, A. *J. Organomet. Chem.* **1983**, *244*, 1.

0020-1669/86/1325-3796$01.50/0

Table I. Observed Infrared Frequencies (cm^{-1}) and Assignments for Dimeric Dimethylaluminum Chloride Assuming D_{2h} Symmetry[a]

	vibrational mode	vapor 298 K	solid 12 K	matrix 12 K
B_{1u}	CH_3 asym str	...	2948 vs	2975 s
	CH_3 sym str	2905 m	2898 m	2910 m
	CH_3 asym def	1440 vw	1440 vw	1443 vw
	CH_3 sym def	1209 m	1202 s	1206 s
	CH_3 rock		758 sh	764 w
	ν_8 Al–C str	700 sh	696 vs	702 vs
B_{2u}	CH_3 asym str	2960 s	2948 vs	2962 s
	CH_3 rock	722 s	723 vs	725 vs
	ν_{13} Al–Cl str	350 m	345 s	351 s
B_{3u}	CH_3 asym str			2955 sh
	CH_3 sym def		1194 sh	1196 vw
	CH_3 rock	613 vw	615 sh	601 w
	ν_{16} Al–C str	585 m	576 s	580 s
	ν_{17} Al–Cl str	317 s	308 vs	317 vs
	overtone (2 × 1440)	~2830 w	~2830 vw	~2830 w
	CH_3 sym def			1202 sh
	CH_4 (ν_3)	3017 w		3030 vs
	CH_4 (ν_4)	1305 w		1310 sh, 1306 s
	additional bands	587 sh	775 sh, 665 sh, 590 sh	715 sh, 675 vw, 495 vw, 374 vw

[a] Key: vw = very weak, w = weak, m = medium, s = strong, vs = very strong, sh = shoulder.

pressure during deposition was less than 2×10^{-5} Torr. Estimated solute to matrix ratios are 1:200–1:600.

IR spectra (4000–300 cm^{-1}) were recorded with a microprocessor-controlled Perkin-Elmer 580B infrared spectrophotometer. The uncertainty in the band positions is estimated to ±1–2 cm^{-1}, and the resolution is better than 5 cm^{-1} down to 350 cm^{-1}. Higher resolution was used for complex band structures.

Argon gas from Norsk Hydro a.s. with a purity of 99.9997% was used without further purification. Dimethylaluminum chloride was synthesized from gallium(III)chloride (Merck, pro analysi) and trimethylaluminum (Alfa Products, 98% electronic grade) as described by Gaines et al.,[14] including repeated vacuum distillations. Methylaluminum dichloride was prepared from trimethylaluminum and aluminum chloride (Fluka AG, purity 99%) by the procedure given by Grosse and Mavity.[15] The melting point of the product was determined to 72.5 °C (literature: 72.7 °C[13]). All chemicals were handled in vacuum or under an inert atmosphere of argon or nitrogen.

Results

Dimethylaluminum Chloride. The IR spectra of gaseous dimeric dimethylaluminum chloride (d-DMAC) at room temperature, pure d-DMAC (s) at 12 K and d-DMAC in solid Ar at 12 K are given in Figure 1. Band positions are listed in Tables I and II. Annealing of the solid sample at 50 K for 1 h did not result in any spectral changes.

The region 800–300 cm^{-1} was studied in more detail for different Knudsen cell temperatures (Figure 2 and Table II). No new bands appeared in the C–H stretching or deformation regions when the cell temperature was raised. Furthermore, intensity changes in both regions were small except those for the methane bands. The abundance of methane increased significantly with the Knudsen cell temperature. Above 500 °C only methane was found in the matrix. The Roman numerals accompanying the bands in Figure 2 and in the corresponding table refer to a scheme for possible reactions of DMAC at elevated temperatures. The reaction scheme, which also comprises MADC, includes dissociation and decomposition of aluminum alkyls. Each compound in the scheme is given a Roman numeral.

All matrices corresponding to Figure 2 were annealed for up to 2 h total time at ca. 40 K. Spectra from the annealing of the matrix prepared with Knudsen cell temperature 400 °C are shown in Figure 3. Band positions are given in Table III. It is seen that the bands attributed to species IX and X vanish by annealing the matrix. This observation was confirmed for all cases where these bands were present in the spectrum of the unannealed matrix.

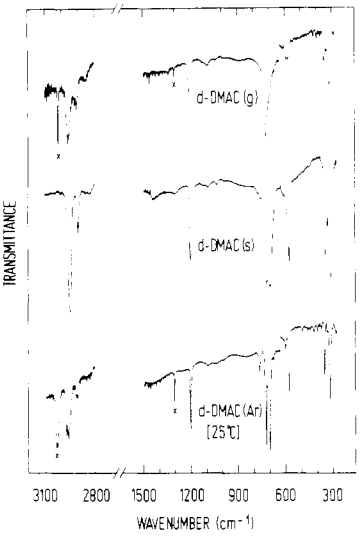

Figure 1. Infrared spectra of dimeric dimethylaluminum chloride in the gas phase (25 °C), in the solid state (12 K) and in solid argon (Knudsen cell at 25 °C, argon deposition rate 6.9 mmol/h). In all figures bands marked with an × are due to methane, and the Knudsen cell temperature is given in square brackets.

Table II. Observed Infrared Frequencies (cm^{-1}) for Matrices Obtained by Varying the Knudsen Cell Temperature for d-DMAC[a]

Knudsen cell temp, °C					interpretation[b]
25	350	375	400	450	
		947 vw	*947* vw	*948* vw	X
764 w	764 w	764 w	764 vw		III
	742 m	*742* m	*742* w		IX
	732 sh	*732* sh	*732* sh	*732* sh	X
725 vs	725 vs	725 vs	726 vs	728 m	III, V
715 sh	719 sh	719 sh	719 w	719 w	IV
702 vs	702 vs	702 vs	702 vs	703 vs	III, V
	695 sh	693 sh	694 m	694 s	IV
			691 sh	691 sh	IX
				678 sh	V
675 vw	674 m	674 s	674 s	674 vs	IV
	660 vw	*653* vw	*653* vw	*653* w	X
				616 vw	XI
601 w	602 m	603 m	603 m	*603* vw	III, IX
	590 sh	588 sh	588 w	588 w	IV
580 s	580 s	580 s	580 m		III
	564 sh	*564* w	*564* m	*564* m	X
	508 sh	508 vw	506 w	510 w	
495 vw	496 s	496 s	496 s	496 sh	IV
			490 sh	489 vs	V
	453 m	*453* m	*453* m	*452* w	IX
	447 sh	447 sh	448 sh	447 sh	IV
			425 vw	*425* w	X
				383 m	V
374 vw	371 m	371 m	371 m	371 m	IV
351 s	351 s	351 m	351 m		III
	342 sh	342 sh	343 vw	344 vw	IV
				324 s	V
317 vs	316 vs	315 vs	315 vs	315 s	III, IV

[a] Band positions in *italics* indicate that the band disappears by annealing the matrix at 40 K. See footnote *a* in Table I. [b] Compound V refers to the trans form of dimeric methylaluminum dichloride.

Methylaluminum Dichloride. Figure 4 contains the matrix spectra of MADC with the Knudsen cell at room temperature, 450, and 550 °C, respectively. Band positions and attributions in Table IV are with reference to the above mentioned reaction scheme. The three argon matrices were all annealed at 40 K. Only in the case of cell temperature 550 °C were changes observed in the spectrum. The four bands attributed to compound X vanished within $^1/_2$ h of annealing. In addition, the intensity of the band at 619 cm^{-1} decreased to about the same intensity as the band

(14) Gaines, D. F.; Borlin, J.; Fody, E. P. *Inorg. Synth.* **1974**, *15*, 203.
(15) Grosse, A. V.; Mavity, J. M. *J. Org. Chem.* **1940**, *5*, 106.

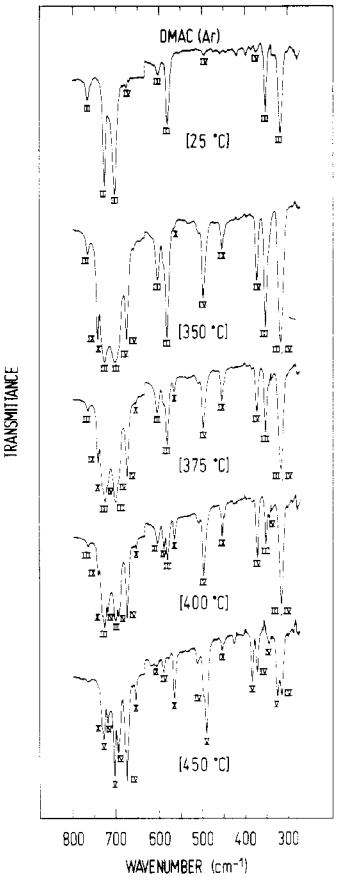

Figure 2. Infrared spectra (800–300 cm^{-1}) of argon matrices obtained by varying the Knudsen cell temperature for dimethylaluminum chloride. The argon deposition rates were ca. 6.5 mmol/h.

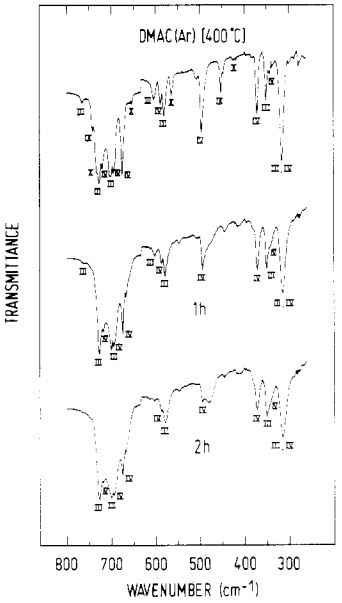

Figure 3. Infrared spectra from annealing at ca. 40 K of the argon matrix prepared with a Knudsen cell temperature of 400 °C for dimethylaluminum chloride. Total time of annealing is indicated.

at 607 cm^{-1} and the shoulder at 490 cm^{-1} became somewhat more distinct.

Discussion

Normal-Coordinate Calculations. Several monomers and chlorine bridged dimers (see supplementary material) have been considered in the interpretation of the complex spectra obtained in the experiments, with elevated Knudsen cell temperatures. Attribution of the individual frequencies to specific molecular

Table III. Observed Infrared Frequencies (cm^{-1}) for a d-DMAC (400 °C) Matrix after Indicated Time of Annealing at 40 K

total time of annealing, h			
0	1	2	interpretation[a]
764 vw	764 vw		III
742 w			IX
732 sh			X
726 vs	726 vs	726 vs	III
719 w	717 w	717 vw	IV
702 vs	700 vs	700 vs	III
694 m	694 m	694 m	IV
691 sh	691 sh	690 sh	IX
674 s	674 s	674 m	IV
	667 vw	667 vw	IV (s)
653 vw			X
603 m	603 w	603 vw	III
588 w	588 w	587 vw	IV
580 m	580 m	578 m	III
564 m			X
	547 vw	547 vw	IV (s)
506 w	506 vw		
496 s	495 m	495 m	IV
490 sh	480 sh	480 m	IV (s)
453 m			IX
448 sh	446 w	446 w	IV
425 vw			X
371 s	371 m	371 m	IV
351 m	350 m	350 m	III
343 vw	342 sh	340 sh	IV
315 vs	314 s	314 s	III, IV

[a] See footnotes to Tables I and II; (s) = solid.

Table IV. Observed Infrared Frequencies (cm^{-1}) for Matrices Prepared by Varying the Knudsen Cell Temperature for MADC[a]

Knudsen cell temp, °C			
25	450	550	interpretation
		3032 s	methane
2960 s	2960 w		CH_3 asym str
2925 w	2925 w	2925 vw	
2905 w			CH_3 sym str
2855 w	2855 w	2855 vw	overtone
1432 vw			CH_3 asym def
		1310 sh	methane
		1305 vs	
		1211 w	
1204 m	1204 m	1204 vw	CH_3 sym def
1190 vw			
		947 vw	X
		735 vw	X
729 w	730 sh		V
		704 m	VI
700 sh	698 m		V
684 vs	685 vs		V
		681 m	VI
676 vs	677 sh		V
		669 m	VI
		653 vw	X
		619 vs	VII, XI
612 w	610 w		V
		607 m	VI
593 w	591 m		V
581 w			V
		564 w	X
		515 w	VI
504 vw	503 m		V
		490 sh	VI
		484 vs	VII
475 sh	475 sh		V
458 vs	460 s		V
		421 m	VII
406 vw	404 m	406 m	V, VI
383 sh	381 m	*383* vw	V, XI
375 m	375 sh		V
335 sh	335 sh		V
322 s	321 s	320 s	V, VI, VII

[a] See footnotes to Tables I and II.

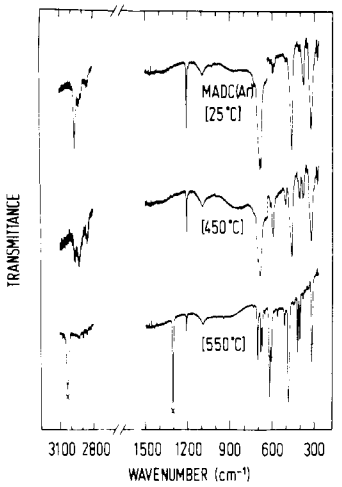

Figure 4. Infrared spectra of argon matrices containing dimeric methylaluminum dichloride obtained with Knudsen cell temperatures of 25, 450, and 550 °C (argon deposition rates 7.3, 8.6, and 7.7 mmol/h, respectively).

species has been supported by harmonic normal coordinate calculations using Wilson's GF matrix method.[16] The applied program is described by Cyvin et al.[17] The point mass used for the methyl groups is 15.035.

Applied geometrical parameters are summarized in the supplementary material. The monomers $(CH_3)_2AlCl$ and $(CH_3)AlCl_2$ were assumed to have trigonal-planar skeletal configurations, i.e. C_{2v} symmetry. Bond distances have not been reported for these monomers. It did, however, benefit from the observation for both Al_2Cl_6 and $(CH_3)_6Al_2$ that the length of the terminal bond in the dimer is equal to the bond length in the monomer.[18,19] For convenience, all dimer geometries employed were compatible with D_{2h} skeletal symmetry.

Valence coordinates are indicated in the supplementary material for the monomers and for the least symmetrical dimer model. Additional coordinates are δ, out-of-plane monomer deformation, and τ, dimer ring puckering.

Symmetry coordinates were constructed by standard methods, and it was assumed to be unnecessary to specify all sets, particularly for the monomers. Dimers with skeletal symmetry D_{2h} have the appropriate linear combinations described by Tomita et al.[20] The coordinates for dimers with skeletal symmetry C_s are given as supplementary material.

There are five redundancies among these 23 symmetry coordinates, four belong to A′ and one to A″. For the dimers with skeletal symmetry C_{2h}, appropriate symmetry coordinates were constructed in an analogous manner.

The normal-coordinate calculations for all the chlorine-bridged dimers are based on the valence force field of Al_2Cl_6, which is well determined.[20] Only four stretch and stretch/stretch interaction force constants of the Al_2Cl_6 force field were modified (vide infra).

Dimethylaluminum Chloride. Reported vibrational spectra of d-DMAC are in agreement with a chlorine-bridged structure,[5-7] as confirmed by gas-phase electron diffraction.[21] The d-DMAC molecule adopts D_{2h} symmetry if the methyl groups are oriented such that the hydrogen atoms are staggered with respect to the bonds radiating from the aluminum atom. Brendhaugen et al.[21] satisfactorily interpreted their electron diffraction data in terms of this molecular structure, although the larger Cl···H vibrational amplitudes indicate rotational freedom of the methyl groups. It may be shown that the skeletal symmetry D_{2h} also is the appropriate point group in the case of torsional tunneling.[3,22] The fundamentals belong to the symmetry species $9A_g + 6B_{1g} + 7B_{2g} + 5B_{3g} + 5A_u + 8B_{1u} + 6B_{2u} + 8B_{3u}$, including the torsions.

Suggested assignments for d-DMAC are given in Table I. The distributions of the five different types of methyl modes among the B species contains several ambiguities. Furthermore, three additional methyl frequencies are expected, namely symmetric stretch in B_u and antisymmetric deformation in B_{2u} and B_{3u}. A particularly interesting feature is the observation in the matrix of three symmetric CH_3 deformations around 1200 cm^{-1} compared to the D_{2h} symmetry prediction of two such bands in the IR spectrum. Our interpretation is that one of the Raman fundamentals is activated due to perturbation of the structure by the surrounding matrix material. Four very weak bands at 715, 675, 495, and 374 cm^{-1} are all attributed to $(CH_3)_3Al_2Cl_3$ (compound IV, Table II).

The most important discrepancy with earlier works concerns the Al–C stretch ν_8. Both Hoffmann[5] and Groenewege[6] found a doublet at around 700 cm^{-1} in the IR spectrum of d-DMAC (l), and they attribute the high-frequency component at 720 cm^{-1} to ν_8 and the component at lower frequency to CH_3 rock. The reverse choice given in Table I cannot be settled conclusively by normal-coordinate calculations. However, skeletal calculations for normal and deuterated d-DMAC show an isotopic shift of 30 cm^{-1} for ν_8. This shift is in reasonable agreement with the strong band at 664 cm^{-1} reported by Gray for the gas-phase IR spectrum of fully deuterated d-DMAC.[7] Besides, the assignment of 725 cm^{-1} as a CH_3 rock corresponds well with the terminal CH_3 rock at 720 cm^{-1} in the trimethylaluminum dimer.[3] The assignments of the other skeletal modes are supported by the normal-coordinate calculations.

Methylaluminum Dichloride. Weidlein[9] has from IR and Raman data of the liquid suggested that the two terminal chlorine atoms of d-MADC are in a trans position, in agreement with a reported X-ray investigation of the solid.[23] With an orientation of the methyl groups such that the hydrogen atoms are staggered relative to the bonds radiating from the aluminum atom, the overall symmetry of the molecule is C_{2h}. All IR-active fundamentals expected above 300 cm^{-1} for this point group are given in Table V except for one antisymmetric methyl deformation (B_u). Note that infrared spectroscopic data for matrix-isolated d-MADC are available from two independent experimental series in the present

Table V. Assignments of Fundamental Vibrations (cm^{-1}) of Dimeric Methylaluminum Dichloride Assuming Trans Configuration

	vibrational mode[a]	liquid[b]	matrix[c] 25 °C	matrix[d] 450 °C	calcd[e]
A_g	ν_1 Al–Cl^t str	495			504
	ν_2 Al–Cl^b str	345			334
	ν_{11} Al–C str	688			666
A_u	CH_3 asym str		2960 s		
	CH_3 asym def		1432 vw		
	CH_3 rock		729 w	728 m	
	ν_{13} Al–Cl^b str	380 m	375 m	383 m	384
B_u	CH_3 asym str		2925 w		
	CH_3 sym str		2905 w		
	CH_3 sym def		1204 m		
	CH_3 rock		684 vs	703 vs	
	ν_8 Al–C str	704 vs	676 vs	678 sh	670
	ν_{16} Al–Cl^t str	485 vs	458 vs	489 vs	493
	ν_{17} Al–Cl^b str	322 m	322 s	324 s	323
	overtone (2 × 1432)		2855 w		

[a] Key: t = terminal; b = bridge. [b] Reference 9. [c] Refers to Figure 4 and Table IV. [d] Refers to Figure 2 and Table II. [e] Force constants are given in Table VIII.

(16) Wilson, E. B.; Decius, J. C.; Cross, P. C. *Molecular Vibrations*; McGraw-Hill: New York, 1955.
(17) Cyvin, J.; Cyvin, B. N.; Brunvoll, J.; Hagen, G. *UNIVAC-ALGOL Program Series for Computation on Vibration-Rotation of Polyatomic Molecules*; Report, Institute of Physical Chemistry, University of Trondheim: Trondheim, Norway, 1968.
(18) Almenningen, A.; Halvorsen, S.; Haaland, A. *Acta Chem. Scand.* **1971**, *25*, 1937.
(19) Shem, Q. Ph.D. Thesis, Oregon State University, 1974.
(20) Tomita, T.; Sjøgren, C. E.; Klæboe, P.; Papatheodorou, G. N.; Rytter, E. *J. Raman Spectrosc.* **1983**, *14*, 415.
(21) Brendhaugen, K.; Haaland, A.; Novak, D. P. *Acta Chem. Scand., Ser. A.* **1974**, *A28*, 45.
(22) Rytter, E., to be submitted for publication.
(23) Allegra, G.; Perego, G.; Immirzi, A. *Makromol. Chem.* **1963**, *61*, 69.

Scheme I

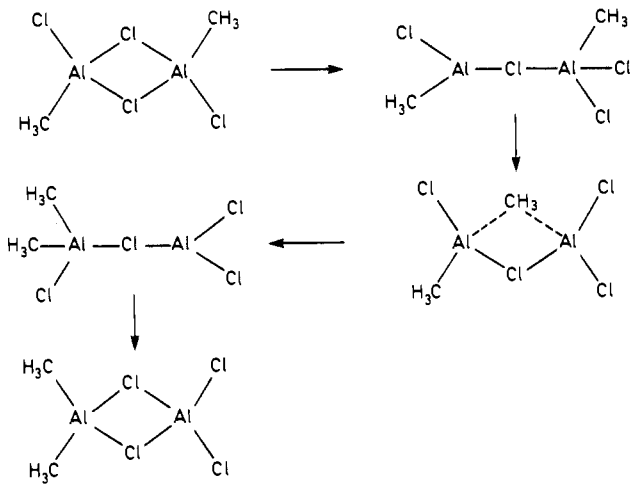

work; the spectra presented in Figure 4 obtained with the room-temperature or 450 °C Knudsen cell procedures for d-MADC and the spectrum in Figure 2 obtained by applying a Knudsen cell temperature of 450 °C for *d-DMAC*. Compound V trapped in the matrix in the latter experiment has frequencies for the skeletal modes in good agreement with the calculated values and those reported by Weidlein. Some significant differences, however, are found for the two matrix spectra compared in Table V, in particular the 31-cm^{-1} shift of the Al–Cl terminal stretch ν_{16}.

The variations in the spectral data for species V (Tables II, IV, and V) are not easily understood, and only some tentative explanations are given:

(1) Solid or aggregated d-MADC caused splitting of bands by neighbor interactions and symmetry reduction.

(2) Structures with an aluminum coordination number higher than four existed, implying that all chlorine atoms participated in bridges (cf. the six-coordinated layer and chain structures of solid $AlCl_3$ and $(CH_3)_2SnCl_2$, respectively).

(3) Not only the trans form of d-MADC was present but also the cis and/or *gem* configurations. Normal-coordinate calculations presented below support and predict the presence of *gem*-V as a band at 594 cm^{-1}, not present in the other isomers, cf. the ca. 592 cm^{-1} band in Table IV. Conversion between isomers may proceed via single- and methyl-bridged[3] intermediates (Scheme I).

(4) There was H···Cl hydrogen bonding between neighboring molecules.

Successive Substitution of Chlorine for Methyl. Experiments were carried out in order to study reactions of the methyl compounds at elevated temperatures, in particular to achieve dissociation. However, it is evident from the spectra in Figures 2–4 that no simple dissociation of the dimers occurred. A scheme with possible high-temperature reactions of the aluminum alkyls in the Knudsen cell therefore was developed. Although other reactions also have been considered (e.g., redistribution), the most important reactions in the scheme are the successive decompositions (cracking)

$$\underset{\text{III}}{6(CH_3)_4Al_2Cl_2} = \underset{\text{IV}}{4(CH_3)_3Al_2Cl_3} + 9CH_4 + Al_4C_3 \quad (1)$$

$$8(CH_3)_3Al_2Cl_3 = \underset{\text{V}}{6(CH_3)_2Al_2Cl_4} + 9CH_4 + Al_4C_3 \quad (2)$$

$$10(CH_3)_2Al_2Cl_4 = \underset{\text{VI}}{8(CH_3)Al_2Cl_5} + 9CH_4 + Al_4C_3 \quad (3)$$

$$12(CH_3)Al_2Cl_5 = \underset{\text{VII}}{10Al_2Cl_6} + 9CH_4 + Al_4C_3 \quad (4)$$

in addition to dissociation into monomers. Redistribution among methyl and chlorine groups, e.g., according to

$$2(CH_2)_4Al_2Cl_2 = \underset{\text{I}}{(CH_3)_6Al_2} + (CH_3)_2Al_2Cl_4 \quad (5)$$

was found *not* to occur. In other words, heating of DMAC or MADC did not produce dimers with higher methyl contents than the starting material. In particular, no trace was found of the well-known matrix spectra[3] of dimeric or monomeric trimethyl aluminum.

All compounds in the reaction scheme, except methane and aluminum carbide, are given a Roman numeral (for completeness: II is $(CH_3)_5Al_2Cl$). The monomers are numbered VIII–XI in the series $(CH_3)_3Al$–$AlCl_3$. For a majority of the dimers a competition between methyl and chlorine bridges can be imagined, rendering several geometrical isomers in principle possible for each stoichiometry. It is, however, assumed that a chlorine bridge is more favorable energetically than a methyl bridge, as suggested by the dissociation enthalpy of Al_2Cl_6, 125 kJ/mol, compared to 85 kJ/mol for $(CH_3)_6Al$.[10,11] The resulting structures for the dimers based on a double-bridged skeleton and four-coordinated aluminum are collected in the supplementary material. Included are the symmetry and normal-coordinate representations for these compounds.

Identification of the individual complexes in the spectra was based on the following points.

(1) By careful inspection of relative intensities, bands in the spectra are grouped together and ascribed to individual monomeric or dimeric compounds (Figures 2–4 and Tables II–IV). Bands that disappear readily by annealing are assigned to monomers. Sets of bands showing the same intensity changes when the Knudsen cell temperature is increased, but not vanishing when the matrix is annealed, are assigned to the same dimeric compound. A careful study of Figure 2 is needed in order to follow the assignments of bands to the different monomers and dimers.

(2) It is assumed that complexes with higher chlorine contents are formed as the Knudsen cell temperature is raised; cf. eq 1–4. This conclusion is a consequence of the observed increased methane concentration in the matrices for the higher cracking temperatures. Note for instance the strong CH_4 bands (marked ×) in Figure 4 when MADC is heated from 450 to 550 °C. Besides, the latter spectrum shows the well-known peaks[20] of aluminum chloride. Thus, it is possible to ascribe sets of peaks to all monomers and dimers that successively can be formed from DMAC to $Al_2Cl_6/AlCl_3$.

(3) The band attributions are supplemented with normal-coordinate calculations (vide infra). The assignments are consistent with systematic changes in force constants. Of particular importance is also the gradual increase of bridge stretching frequencies in the series $(CH_3)_{6-n}Al_2Cl_n$, n = 2–6, discussed in further detail below. This shift is clearly seen in Figure 2 where there appears to be a shift from 351 to 371 to 383 cm^{-1} for complexes III–V and a further shift (Figure 4) to 406 and 421 cm^{-1} for VI and VII.

The assignments are complicated by overlap of bands, particularly extensive in the CH_3 stretching and deformation regions. These regions therefore are disregarded. The interpretation of the spectra is consistent with the following high-temperature reaction sequences:

$$\begin{array}{lccccc}
\text{d-DMAC} & & & & & \\
 & (CH_3)_4Al_2Cl_2 & \longrightarrow & (CH_3)_3Al_2Cl_3 & \longrightarrow & (CH_3)_2Al_2Cl_4 \\
 & \text{III} & & \text{IV} & & \text{V} \\
 & \downarrow & & \downarrow & & \downarrow \\
 & (CH_3)_2AlCl & & (CH_3)_2AlCl + (CH_3)AlCl_2 & & (CH_3)AlCl_2 \\
 & \text{IX} & & \text{IX} \quad \text{X} & & \text{X}
\end{array} \quad (6)$$

$$\begin{array}{lccccc}
\text{d-MADC} & & & & & \\
 & (CH_3)_2Al_2Cl_4 & \longrightarrow & (CH_3)Al_2Cl_5 & \longrightarrow & Al_2Cl_6 \\
 & \text{V} & & \text{VI} & & \text{VII} \\
 & \downarrow & & \downarrow & & \downarrow \\
 & (CH_3)AlCl_2 & & (CH_3)AlCl_2 + AlCl_3 & & AlCl_3 \\
 & \text{X} & & \text{X} \quad \text{XI} & & \text{XI}
\end{array} \quad (7)$$

Monomers. Table VI contains observed and calculated frequencies and assignments for the skeletal modes of the monomers

Table VI. Assignments of Fundamental Skeletal Frequencies (cm^{-1}) of Monomeric Dimethylaluminum Chloride and Methylaluminum Dichloride

vibrational mode		obsd[a]	calcd[b]	PED[c]
		$(CH_3)_2AlCl$ (IX)		
A_1	ν_1 sym Al–C str	603 w	603	88r + 23R
	ν_2 Al–Cl str	453 m	453	74R + 13r
	ν_3 sym def	...	162	95 bend
B_1	ν_4 out-of-plane def	...	188	100τ
B_2	ν_5 asym Al–Cl str	691 sh[d]	693	98r
	ν_6 asym def	...	143	98β
	CH_3 rock	742 m		
		$(CH_3)AlCl_2$ (X)		
A_1	ν_1 Al–C str	653 w	653	94R + 14r
	ν_2 sym Al–Cl str	425 w	425	85r + 6R
	ν_3 sym def	...	142	95 bend
B_1	ν_4 out-of-plane def	...	175	100τ
B_2	ν_5 asym Al–Cl str	564 m	564	96r
	ν_6 asym def	...	146	96β
	CH_3 rock	732 sh		

[a] Values from Table II. [b] Valence force fields; see supplementary material. [c] Potential energy distribution of diagonal terms. Values less than 5 are omitted. [d] See comment in text.

m-DMAC and m-MADC. The assignments are essentially based on a comparison with $(CH_3)_3Al$ and $AlCl_3$.[3,20] Antisymmetric stretching modes should be situated at a higher frequency than symmetric ones, the intense ν_{rock} around or slightly above 700 cm^{-1} and higher than ν_{Al-C}, and $\nu_{Al-C} > \nu_{Al-Cl}$ on an average for each molecule. The experimental limitation to stretching modes of the skeleton and the excessive number of force constants necessitated approximations and transfer of adequate force constants from the monomers $(CH_3)_3Al$ and $AlCl_3$,[3,20] as indicated in the supplementary material.

For $(CH_3)_2AlCl$ the force constants f_{Al-Cl} and $f_{Al-C,Al-Cl}$ were adjusted to obtain a perfect fit for ν_1 and ν_2. It follows that the antisymmetric Al–C stretch (ν_5) is calculated to be 693 cm^{-1}. Due to multiple overlap around 700 cm^{-1} it is difficult to separate bands in this region, but the spectra of d-MADC (400 °C) and d-DMAC (450 °C) do show a shoulder at 691 cm^{-1}. It is impossible, however, to decide whether this shoulder disappears by annealing. Nevertheless, a verification of the expected band position comes from the closeness to ν_8 for the dimers III and IV (702 and 694 cm^{-1}, Table VII). Regarding the methyl rockings, more than one IR active mode of this type is predicted for both m-DMAC and m-MADC, but only one strong CH_3 rock is observed, as for m-TMAL.[3]

The calculations indicate that the assumption of transferability of the Al–C force constant among the three methyl containing monomers is reasonable. On the other hand, it was impossible to obtain consistent force fields without an increase in the Al–Cl stretching constant by substitution of a methyl group with a chlorine atom. Unfortunately, this inductive effect cannot be verified by molecular geometries as such data are not available for the mixed methyl–chlorine monomers. The observed increase of the Al–Cl bond strength, however, is compatible with ab initio SCF MO calculations.[24] Population analysis show that the main bonding interactions in the Al–Cl bond involve all the valence orbitals on aluminum and the 3p orbitals on chlorine, with the Al(3s)–Cl(3p) component of the overlap population increasing appreciably from $(CH_3)_2AlCl$ to $AlCl_3$.

A systematic variation of f_{Al-Cl} also can be rationalized by an increasing partial charge on the aluminum atom as the methyl groups are substituted with chlorine atoms, causing an enhanced ionic resonance energy of the Al–Cl bond. This explanation has been suggested for the significant decrease in the C–F bond length in the series $CH_3F > CH_2F_2 > CHF_3 > CF_4$.[25] Similar arguments have been put forth regarding the Ga–Cl distances and force constants in the methylchlorogallate ions $(CH_3)_{4-n}GaCl_n^-$ (n = 0–4).[26]

Dimers. Observed and calculated frequencies and assignments for the skeletal modes are listed in Table VII. The experimental values for $(CH_3)_4Al_2Cl_2$ (d-DMAC), $(CH_3)_3Al_2Cl_3$ and *trans*-$(CH_3)_2Al_2Cl_4$ (d-MADC) are obtained from the matrix spectra based on d-DMAC, whereas d-MADC at 450 °C gives data for *gem*-$(CH_3)_2Al_2Cl_4$ and at 550 °C gives data for $(CH_3)Al_2Cl_5$ and Al_2Cl_6. The numbering of the fundamentals refers to the distribution in the D_{2h} symmetry group.[20] Standard symmetry correlations, see supplementary materials, may be applied to achieve the distribution of the skeletal modes in the C_{2h} and C_s symmetry groups using the D_{2h} numbering. The assignments for the intermediate compounds follow essentially from the results for $(CH_3)_6Al_2$,[3] *trans*-$(CH_3)_4Al_2Cl_2$ (Table I), $(CH_3)_2Al_2Cl_4$ (Table V), and Al_2Cl_6.[20] Each terminal AlXY group gives rise to characteristic group frequencies as is expected from the isolation effect of the bridge. This phenomenon is discussed in detail in the last section.

The Al_2Cl_6 valence force field has been transferred to compounds III–VI except for the terminal stretch, bridge stretch, terminal stretch/stretch interaction, and bridge stretch/stretch interaction. Values of these force constants for compounds IV–VI were derived from the force fields of Al_2Cl_6,[20] $(CH_3)_4Al_2Cl_2$, and $(CH_3)AlCl_2$ by considering each compound as consisting of two molecular halves connected by the chlorine bridge:

(1) The bridge stretch/stretch force constant was calculated by the equation

$$f = \frac{1}{4}[n\, f_{RR}(\text{d-DMAC}) + (4 - n)\, f_{RR}(Al_2Cl_6)] \qquad (8)$$

where n is the number of CH_3 groups in the molecule and f_{RR}(d-DMAC) and $f_{RR}(Al_2Cl_6)$ are bridge stretch/stretch constants.

(2) With two CH_3 groups on the Al atom, the remaining force constants were transferred from d-DMAC.

(3) With two terminal Cl atoms on the Al atom, the remaining force constants were transferred from Al_2Cl_6.

(4) With one CH_3 group and one terminal Cl atom on the Al atom, the Al–C force constant was transferred from d-DMAC and the terminal Al–Cl constant from m-MADC. The Al–Cl bridge and terminal stretch/stretch constants equal the mean values of the respective force constants in d-DMAC and Al_2Cl_6.

The skeletal stretching force fields for the dimers are summarized in Table VIII. By the described procedure, only five independent stretching force constants of the two parent compounds d-DMAC (III) and m-MADC (X) are varied in order to fit 37 frequencies of four dimers and one monomer (not counting the well-established Al_2Cl_6 parameters). The good agreement between observed and calculated frequencies supports the applied transferring method for the valence force constants. More importantly, the whole high-temperature reaction scheme and the assignments are verified.

Additional calculations reveal that the skeletal modes of the cis and trans forms of $(CH_3)_2Al_2Cl_4$ (V) have almost identical values. However, *cis*-V is not considered in the present work as the trans form has been reported to be the more stable of the two.[9,23] The normal-coordinate analyses show that the *gem* isomer is expected to have an IR-active band at 594 cm^{-1} (ν_1, Al–C stretch). Note that two of the d-MADC spectra *do* show a ~590-cm^{-1} band (Table IV). Therefore a tentative assignment of *gem*-V fundamentals has been included in Table VII. It is seen that additional support for the existence of the *gem*-isomer is found in the IR activation of ν_2 and ν_{11}.

It often is assumed that bond energies are proportional to the force constants.[27] Hence, from the skeletal stretching force

(24) Lappert, M. F.; Pedley, J. B.; Sharp, G. J.; Guest, M. F. *J. Chem. Soc., Faraday Trans. 2* **1976**, *72*, 539.
(25) Huheey, J. E. *Inorganic Chemistry*, 3rd ed.; Harper: New York, 1983; p 252.
(26) Haaland, A.; Weidlein, J. *Acta Chem. Scand., Ser. A.* **1982**, *A36*, 805.
(27) Nakamoto, K. *Infrared and Raman Spectra of Inorganic and Coordination Compounds*; Wiley: New York, 1978.

Table VII. Assignments of Fundamental Skeletal Frequencies (cm^{-1}) for Compounds in the Series $(CH_3)_{6-n}Al_2Cl_n$ (n = 2–6)[a]

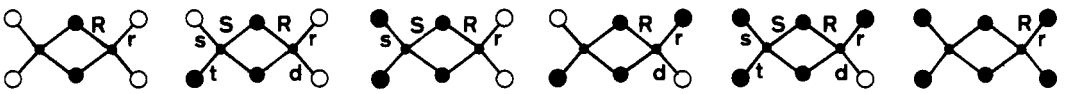

	III (D_{2h})		IV (C_s)		*gem*-V (C_{2v})		*trans*-V (C_{2h})		VI (C_s)		VII (D_{2h})	
Mode	obs[b]	calc PED[c]	obs	calc PED	obs[d]	calc PED	obs	calc PED	obs	calc PED	obs	calc PED
ν_1	(588 vs)	594 102r	588 w	591 48d+48r	591 m	594 95 r	(495 m)	504 78r+12R	515 w	509 54r+13t+11s	(523 m)	508 84r+25R
ν_2	(330 s)	322 101R	344 vw	331 104S+12R	335 sh	330 88S+16R	(345 vs)	334 114R	-	335 59R+46S	(342 vs)	339 86R
ν_6	(247 m)	256 168R	-	261 98R+74S	-	265 108R+66S	(266 vs)	269 176R	-	275 99R+78S	(284 m)	281 123R
ν_{11}	(713 m)	701 97r	674 vs	670 88s+16t	610 w	624 103s	(688 s)	666 90d+14r	607 m	620 52s+51t	(612 w)	616 94r
ν_8	702 vs	705 96r	694 s	704 52d+52r	698 m	701 104r	678 sh	670 88d+16r	669 m	667 89d+14r	619 vs	622 92r
ν_{13}	351 s	355 115R	371 m	370 56S+34R	404 m	388 64S+26R	383 m	384 88R	406 m	401 53S+34R	421 m	414 112R
ν_{16}	580 s	587 105r	496 s	496 78t+13s+11S	503 m	489 81s+27S+16bend	489 vs	493 78r+14d	490 sh	489 30s+28t+26r+19S	484 vs	482 98r+20R
ν_{17}	317 vs	320 105R+40bend	314 s	319 117R+15S+30bend	321 s	318 116R+28bend+16S	324 s	323 128R+45bend	320 s	321 62R+58S+35bend	320 s	316 85R+30bend
CH_3 rock	764 w, 725 vs, 601 w		726 vs, 719 w, 691 sh		730sh,685vs		728 m, 703 vs		704 m, 681 m			

[a] Key: (○) CH_3; (●) Cl; (•) Al. [b] Frequencies in parentheses are reported Raman values. $(CH_3)_4Al_2Cl_2$ (l) by Hoffman[5] and Groenewege,[6] $(CH_3)_2Al_2Cl_4$ (l) by Weidlein, and Al_2Cl_6 by Tranquille.[28] [c] Values less than 10 in the potential energy distributions are omitted. [d] Tentative assignments of selected bands from the d-MADC (450 °C) argon matrix.

Table VIII. Valence Force Fields for Dimeric Methylaluminum Chlorides

	force constant,[a] mdyn/Å					
	$(CH_3)_4Al_2Cl_2$ (III)	$(CH_3)_3Al_2Cl_3$ (IV)	$(CH_3)_2Al_2Cl_4$ (*gem*-V)	$(CH_3)_2Al_2Cl_4$ (*trans*-V)	$(CH_3)Al_2Cl_5$ (VI)	Al_2Cl_6 (VII)
			Stretch			
f_d	2.43	2.43	2.43	2.43	2.43	2.759
f_r				2.41	2.41	
f_s			2.759		2.759	
f_t		2.41		2.41		
f_R	0.93	0.93	0.93	1.05	1.05	1.177
f_{RS}		1.05	1.177		1.177	
			Stretch/Stretch			
f_{dr}	0.20	0.20	0.20	0.25	0.25	0.295
f_{st}		0.25	0.295		0.295	
f_{RS}	0.17	0.20	0.23	0.23	0.26	

[a] Corresponding valence coordinates are included in the supplementary material. The rest of the constants are transferred from Al_2Cl_6.[20]

constants in Table VIII it is predicted that the *gem* configuration is the more stable as the weakening effect of a methyl group on a neighboring Al–Cl terminal bond is avoided. This fact does not contradict the observation of only the trans isomer for matrix-isolated d-MADC produced from DMAC. If recombination of $(CH_3)AlCl_2$ monomers is an important step in the high-temperature reaction mechanism, no *gem* isomers are expected to be formed at all. A further requirement is that no trans–*gem* conversion (see Scheme I) takes place when DMAC is the starting material.

It has been mentioned that one particular spectral feature has been of great value in the identification of the individual dimers. The ν_{13} fundamental, which is a bridge mode, is shifted smoothly toward higher frequency by substituting a methyl group with a chlorine atom, reflecting the increase of the bridge stretching force constant (Table VIII). In this context it is pertinent to recall the observed shortening of the Al–Cl bridge bond in the dimers: $(CH_3)_4Al_2Cl_2$ (g), 2.303 Å;[21] $(CH_3)_2Al_2Cl_4$ (s), 2.26 Å;[23] Al_2Cl_6 (g), 2.252.[19] Brendhaugen et al.[21] attributed this contraction to an increase of the acceptor strength of the aluminum atom when the terminal methyl groups are exchanged with the more electronegative chlorine atoms. The ab initio calculations[24] indicate that Cl(3p) → Al(3d) back-bonding is an important factor in this respect. The effect on the bridge force constant parallels the results for f_{Al-Cl} in the monomeric compounds.

As a concluding remark in this section the difference between the high temperature reactions of chlorine-bridged and methyl-bridged dimers is emphasized. The dissociation of d-TMAL (eq 1) takes place more readily,[3] indicating that the dissociation enthalpies of all the chlorine-bridged dimers are higher. In fact, a series of increasing stability of the dimers

$$(CH_3)_6Al_2 < (CH_3)_4Al_2Cl_2 < (CH_3)_2Al_2Cl_4 < Al_2Cl_6 \qquad (9)$$

is predicted from the summed stretching force constants of the bridges: 3.0,[3] 3.72, 4.20, and 4.71 mdyn/Å, respectively. An attempt to add all the stretching force constants of both monomers and dimers does not give the same smooth trend, but the span is still ca. 1.6 mdyn/Å in favor of $(CH_3)_6Al_2$ compared to Al_2Cl_6 dissociation. These results are in agreement with mass spectroscopic and photoelectronic studies of the compounds.[24,29,30] Furthermore, the above trend gives a thermodynamic rationale for the effect of alkylaluminum chlorides as alkylation or reduction agents:

$$R_{6-n}Al_2Cl_n + MCl_m \rightarrow R_{5-n}Al_2Cl_{n+1} + RMCl_{m-1} \qquad (10)$$

$$R_{6-n}Al_2Cl_n + MCl_m \rightarrow R_{5-n}Al_2Cl_{n+1} + MCl_{m-1} + R^{\bullet} \qquad (11)$$

Characteristic Frequencies. Although it has been possible to identify series of monomeric and dimeric alkylaluminum chlorides from infrared spectra and perform frequency assignments, it remains to be verified to what extent characteristic frequencies or group frequencies exist for these compounds. The line diagram in Figure 5 has been prepared to assist in such an analysis. Data included in the diagram are matrix frequencies from Tables VI and VII, as well as those from the previous report on the pure alkylaluminum compounds,[3] and Raman frequencies from the literature. All eight skeletal stretching modes are depicted for the dimers while only the highest stretching frequency of the monomers can be systemized in this way.

It is evident from the figure that most fundamentals fall within narrow frequency ranges and can be regarded as group frequencies, either characteristic of the terminal AlXY (X, Y = Cl or Me) group or the AlX_2Al type of bridge. Furthermore, according to the potential energy distributions, each group of frequencies can

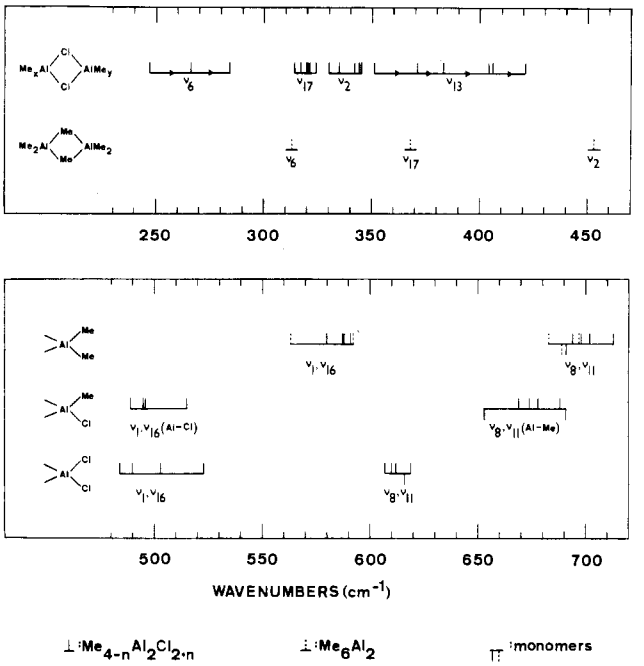

Figure 5. Skeletal stretching frequencies of methylaluminum chlorides.

be described in terms of Al–Cl or Al–Me stretching of terminal or bridging bonds.

Before some of the details of Figure 5 are discussed, it is pointed out that for all the dimers *individually* the following ordering of fundamental modes is valid:

$$\nu_8 > \nu_{11} > \nu_1 > \nu_{16} > \nu_{13} > \nu_2 > \nu_{17} > \nu_6 \qquad (12)$$

These relations also are good for Ga_2Cl_6 with the modification $\nu_{13} \approx \nu_2$ and for Al_2Br_6 and Al_2I_6 with $\nu_6 > \nu_{17}$.[31,32] If all $AlCl_2Al$-bridged molecules are considered *jointly* (or the $AlMe_2Al$-bridged molecules), the ordering becomes

$$\nu_8, \nu_{11} > \nu_1, \nu_{16} > \nu_{13} > \nu_2 > \nu_{17} > \nu_6 \qquad (13)$$

With the alteration that overlap may occur between the ν_{13}, ν_2, and ν_{17} regions, the last equation can be applied to *any* mixture of double-bridged alkylaluminum chlorides. In particular, the terminal stretching frequencies of one molecule will always be higher than the bridging frequencies of any other molecule. A similar relationship applies to the symmetric and antisymmetric stretching modes of the AlX_2 terminal groups. An antisymmetric mode (ν_8, B_{1u}; ν_{11}, B_{2g}) has always a higher energy than the symmetric modes (ν_1, A_g; ν_{16}, B_{3u}) of any alkylaluminum chloride.

A closer inspection of the terminal frequencies in Figure 5 and of the underlying material reveals a number of interesting features:

(1) The antisymmetric ν_{Al-Me^t} (ν_8, ν_{11}) at 690 ± 25 cm^{-1} is slightly higher (~25 cm^{-1}) if the neighboring terminal ligand is methyl rather than chlorine. This shift probably is due to mass coupling.

(2) The symmetric ν_{Al-Cl^t} (ν_1, ν_{16}) at 500 ± 25 cm^{-1} is almost independent of the type of neighboring ligand. For instance, a substitution of methyl for one terminal chlorine induces a lower remaining Al–Cl force constant, but the result is neutralized by a lighter end group.

(3) ν_{Al-Me^t} is nearly the same regardless of the type of bridging atom. A small shift toward lower frequencies, however, seems to be evident for the antisymmetric stretch (ν_8, ν_{11}) when a methyl bridge is substituted for a chlorine bridge.

Apart from the characteristic Al–Cl^t frequency around 500 cm^{-1}, and possibly the $AlMe_2^t$ frequency at ca. 585 cm^{-1}, the terminal modes unfortunately are in a region of the spectrum that

(28) Tranquille, M.; Fouassier, M. *J. Chem. Soc., Faraday Trans. 2* **1980**, *76*, 26.
(29) Tanaka, J.; Smith, S. R. *Inorg. Chem.* **1969**, *8*, 265.
(30) Bocharev, V. N.; Belokon', A. I.; Fedorovich, A. D. *Zh. Obshch. Khim.* **1980**, *50*, 586; *J. Gen. Chem. USSR (Engl. Transl.)* **1980**, *50*, 472.
(31) Sjøgren, C. E.; Klæboe, P.; Rytter, E. *Spectrochim. Acta. Part A* **1984**, *A40*, 457.
(32) Klæboe, P.; Rytter, E.; Sjøgren, C. E. *J. Mol. Struct.* **1984**, *113*, 213.

is scattered with rocking modes. The vibrations of the bridge, however, are situated in a part that is much cleaner. Some very useful rules thus may be added (see Figure 5):

(4) $\nu_{Al-Me^b} > \nu_{Al-Cl^b}$. This relation is valid for all the four bridging modes separately. The mass change is evidently responsible for the trend.

(5) $\nu_{17}(Al-Cl^b) = 320 \pm 10$ cm^{-1} and $\nu_2(Al-Cl^b) = 340 \pm 10$ cm^{-1}. The first of these bands is always strong in the IR region and the second is dominant in the Raman region. Note that the AlCC bend may be present in the same spectral region.

(6) ν_6 and ν_{13} increase gradually when terminal methyl groups are substituted by chlorine, i.e. in the series $Me_{6-n}Al_2Cl_n$ (n = 2-6), clearly showing the inductive effect of the alkyl group.

In conclusion, the systematic variations of the skeletal frequencies and the force fields build a strong case for the interpretation of the high-temperature reactions in terms of successive chlorine substitution.

Acknowledgment. The authors are grateful to Professor H.A. Øye for his encouragement and interest in the work. Financial support from the Royal Norwegian Council for Scientific and Industrial Research is acknowledged.

Registry No. I, 15632-54-9; II, 95974-48-4; III, 14281-95-9; IV, 12542-85-7; *gem*-V, 103731-98-2; *trans*-V, 103774-90-9; VI, 103731-99-3; VII, 13845-12-0; VIII, 75-24-1; IX, 1184-58-3; X, 917-65-7; XI, 7446-70-0.

Supplementary Material Available: Tables of the structure, symmetry, and normal-coordinate representation of the skeletal modes for $(CH_3)_{6-n}Al_2Cl_n$, applied geometrical parameters for methylaluminum chlorides, simplified valence force fields for monomeric alkylaluminum chlorides, and symmetry coordinates for a double-bridged $A_2X_3YZ_3$ model, figures showing valence coordinates for the AX_2Y and double-bridged $A_2X_2YZ_3$ models, and a correlation diagram for symmetry reductions from D_{2h} to C_{2h} and C_s (5 pages). Ordering information is given on any current masthead page.

Contribution from the Departamento de Química Inorgánica, Facultad de Química, Universidad de Sevilla, 41012 Sevilla, Spain, Departamento de Química Inorgánica, Facultad de Ciencias, Universidad de Cádiz, Cádiz, Spain, Instituto de Química Inorgánica Elhúyar, CSIC, Serrano 113, Madrid, Spain, and Facultad de Químicas, Universidad Complutense, 28040 Madrid, Spain

Formation of Zwitterionic Ligands, $ROC^-(^+PMe_3)S^-_2$, by Nucleophilic Attack of PMe_3 on Coordinated Xanthates. X-ray Structure of $MoO[S_2C(PMe_3)O$-*i*-Pr-*S*,*S*′$](CS_2CO$-*i*-Pr-*S*,*S*′,*C*$)$†

Ernesto Carmona,*‡ Agustín Galindo,‡ Enrique Gutiérrez-Puebla,*§ Angeles Monge,§ and Carmen Puerta‖

Received February 26, 1986

New oxo complexes of composition $MO(S_2COR)_2(PMe_3)$ (M = Mo, W; R = Me, Et, *i*-Pr) have been synthesized by the reactions of $MOCl_2(PMe_3)_3$ with the potassium salts of the xanthate ligands. NMR studies (^1H, ^{13}C, ^{31}P) show the existence in the molecules of these complexes of the zwitterionic ligands $^-S_2C^-(^+PMe_3)OR$, formed by nucleophilic attack of trimethylphosphine on the carbon atom of the CS_2 moiety. This has been confirmed by an X-ray study, carried out on the molybdenum isopropyl derivative, which shows in addition that the second xanthate group displays an unusual coordination, acting as an η^3 ligand, bonded to molybdenum through the two sulfur atoms and the carbon atom of the CS_2 group. The crystals are orthohombic, *Pbca*, with unit cell constants a = 13.168 (7) Å, b = 13.622 (9) Å, c = 21.732 (6) Å, and D_{calcd} = 1.57 g cm^{-3} for Z = 8. The structure was refined to an R value of 0.034 by using 2446 independent observed reflections. The molybdenum atom is in a distorted-square-pyramidal environment, with a Mo-O separation of 1.668 (3) Å, lying 0.83 Å above the basal plane formed by the four sulfur atoms of the xanthate ligands.

Introduction

The interest in the bioinorganic chemistry of molybdenum and the implication of Mo-S bonding in the active site of the iron-molybdenum protein of nitrogenase have originated numerous studies on molybdenum complexes of dithio acid ligands.[1] In the course of the past few years, we have become interested in the synthesis and properties of molybdenum and tungsten complexes containing this type of ligand[2,3] and reported recently that the interaction of the oxo derivatives $MOCl_2(PMe_3)_3$ with various dialkyldithiocarbamates, $^-S_2CNR_2$, yields the new complexes $MO(S_2CNR_2)_2(PMe_3)$ (R = Me, Et) as shown in eq 1. As an

$$MOCl_2(PMe_3)_3 + 2NaS_2CNR_2 \rightarrow MO(S_2CNR_2)_2(PMe_3) + 2PMe_3 + 2NaCl \quad (1)$$

extension of these studies, the preparation of the alkyl xanthate (^-S_2COR) analogues by a similar procedure has been attempted, and the results are reported in this paper. While the reactions of the oxo complexes with KS_2COR (R = Me, Et, *i*-Pr) afford monomeric compounds of the expected analytical composition, namely $MO(S_2COR)_2(PMe_3)$, NMR studies (^1H, ^{13}C, and ^{31}P) and an X-ray analysis carried out on the molybdenum isopropyl derivative reveal that (i) the PMe_3 ligand is not bonded directly to the metal atom but instead forms a bidentate zwitterionic ligand, $^-S_2C^-(^+PMe_3)OR$, and (ii) the second xanthate group is acting as a tridentate ligand, bonded to molybdenum through the two sulfur atoms and the carbon atom of the CS_2 unit, in a way that resembles a π-allyl-metal interaction.

Results and Discussion

Synthesis of the Complexes $MO[S_2C(PMe_3)OR](S_2COR)$ (M = Mo, W; R = Me, Et, *i*-Pr). Interaction of the oxo compounds $MOCl_2(PMe_3)_3$ with potassium *O*-alkyl xanthates, KS_2COR (R = Me, Et, *i*-Pr), in tetrahydrofuran (THF), at room temperature, gives yellow crystalline complexes of analytical composition

† Dedicated to Professor Usón on his 60th birthday.

‡ Universidad de Sevilla.
§ Instituto de Química Inorgánica Elyhüyar and Universidad Complutense de Madrid.
‖ Universidad de Cádiz.

(1) (a) McDonald, J. W.; Corbin, J. L.; Newton, W. E. *J. Am. Chem. Soc.* **1975**, *97*, 1970. (b) Newton, W. E.; Chen, G. J.; McDonald, J. W. *J. Am. Chem. Soc.* **1978**, *100*, 1318. (c) Maata, E. A.; Wentworth, R. A. D.; Newton, W. E.; McDonald, J. W.; Watt, G. D. *J. Am. Chem. Soc.* **1978**, *100*, 1320.
(2) Carmona, E.; Sánchez, L.; Marín, J. M.; Proveda, M. L.; Atwood, J. L.; Priester, R. D.; Rogers, R. D. *J. Am. Chem. Soc.* **1984**, *106*, 3214. Carmona, E.; Doppert, K.; Marín, J. M.; Poveda, M. L.; Sánchez, L.; Sánchez-Delgado, R. *Inorg. Chem.* **1984**, *23*, 530.
(3) (a) Carmona, E.; Galindo, A.; Sánchez, L.; Nielson, A. J.; Wilkinson, G. *Polyhedron* **1984**, *3*, 347. (b) Carmona, E.; Sánchez, L.; Poveda, M. L.; Jones, R. A. Hefner, J. G. *Polyhedron* **1983**, *2*, 797.

0020-1669/86/1325-3804$01.50/0